

PHYSICAL PROPERTIES OF HOT WALL DEPOSITED $\text{Sn}_{1-x}\text{Pb}_x\text{S}$ THIN FILMS

V. F. Gremenok¹, V. A. Ivanov¹, H. Izadneshan¹, V. V. Lazenka², A. Bakouie³

¹State Scientific and Production Association “Scientific-Practical Materials Research Centre of the National Academy of Sciences of Belarus”,
P. Brovka Street 19, 220072 Minsk, Belarus

²Institute for Nuclear and radiation physics (IKS),
KU Leuven, Celestijnenlaan 65/84, 3001 Leuven, Belgium

³Department of Physics, Marvdasht Branch, Islamic Azad University, Marvdasht, Iran
4-Tarbiat Modares University, Teheran, Iran

vasil@physics.by

PACS 73.50.-h

Thin films and nanorods of $\text{Sn}_{1-x}\text{Pb}_x\text{S}$ ($0.00 \leq x \leq 0.45$) with orthorhombic crystal structure and *c*-axis oriented perpendicular to the substrate surface were grown by hot wall vacuum deposition (HWVD) method. The nanorods grew via a self consuming vapor–liquid–solid (VLS) mechanism by means of Sn-droplets onto the surface of an underlying thin film. The former one consists of stacked blocks with their *c*-axis always parallel to the growth direction. However, each block is alternately rotated around the [001] against its underlying and subsequent one. As revealed by composition analysis, there is no composition gradient across or within the nanorods and the underlying film. The rods were about 500 nm high and 250 nm in diameter. The droplet at the top of rods consists of Sn with small trace of Pb and S. The density of rods, arranged like a lawn, depends on the metal ratio and substrate temperature. The as-grown $\text{Sn}_{1-x}\text{Pb}_x\text{S}$ samples showed p-type electrical conductivity. Increasing the lead atom concentration results in a decreased Seebeck coefficient and lower conductivity.

Keywords: Hot Wall Deposition, Physical Properties, Thin Films.

Received: 26 August 2014

Revised: 29 September 2014

1. Introduction

Novel inexpensive materials with high photovoltaic efficiencies are needed for thin film solar cells, replacing most extensively studied materials as CdTe and $\text{Cu}(\text{In,Ga})\text{Se}_2$. Recently, a considerable effort has been invested to gain a better and deeper understanding of physical properties of the lead tin chalcogenide semiconductors because of their potential application in electrical and photonic devices [1-4]. The most interesting candidates are (Sn,Pb)S mixed crystals. SnS has an orthorhombic structure and consists of double layers weakly bound to each other, while PbS has a cubic structure. The crystal structures of SnS–PbS bulk materials have been examined and linear relationships between cell parameters *a*, *b* and *c* and composition have been established [5-7]. Both PbS (optical band gap of 0.4 eV) and SnS (optical band gap of 1.1–1.7 eV) semiconductors are promising materials in photovoltaic, infrared detection and other optoelectronic devices. To evaluate these materials for such applications, their microstructure, optical, electrical properties should be thoroughly understood. In addition, lead and tin containing sulfides in photovoltaic structures would

decrease the production costs of solar cells, because the materials involved are cost effective, abundant in nature, and somewhat less-toxic.

A few techniques have been applied for the preparation of $\text{Sn}_{1-x}\text{Pb}_x\text{S}$ thin films. The first report was by Thangaraju and co-workers [8], who prepared PbSnS_2 films by a spray pyrolysis method. Unuchak et al. deposited PbSnS_2 thin film by thermal evaporation [4]. The preliminary structural and optical characteristics have been reported.

New approaches and various techniques must be developed to control the deposition of photoactive materials with minimum density of defects, so that carrier generation, transport, and collection are optimized. Shape and size of nanostructures have considerable influence on physical properties of such semiconductors especially for the phonons due to the lattice part of the thermal conductivity for which nanorods constitute an important class of corresponding 1D nanostructures [9-11]. At the same time, bicontinuous morphology is necessary to decrease the distance needed for excitons to diffuse to interfaces and to allow charges to efficiently diffuse to electrode interfaces. Nanorods constitute an important class of 1D nanostructure and can also act as active components in devices. Previously, much effort has been made to develop novel methods for fabrication of nanostructured chalcogenide semiconductors [12]. Among these technologies, the vapor-liquid-solid (VLS) method seems to be the most successful for generating nanocrystalline nanowires with relatively large quantities [13,14].

In our continuing effort to prepare the SnS-PbS semiconductor films, we have used a hot wall vacuum deposition (HWVD) method. Among the various thin films deposition techniques, HWVD has become a popular and reliable synthesis for films preparation [15-21]. This deposition technology yields high quality thin films with smooth surfaces grown under conditions very close to a quasi thermal equilibrium. The high quality of the electrical and optical properties thin films of the different II-VI materials produced by this method didn't require additional post-growth heat treatments [22,23].

Here, we report on the preparation of $\text{Sn}_{1-x}\text{Pb}_x\text{S}$ thin films and nanorods by the hot wall vacuum deposition of bulk materials onto glass substrates using different synthetic parameters. Microstructure and electrical properties of the as deposited materials are also described.

2. Experimental details

The polycrystalline $\text{Sn}_{1-x}\text{Pb}_x\text{S}$ ($0.00 \leq x \leq 0.45$) ingots used as targets were synthesized by reaction of Sn, S of high purity 99.999% and natural galena (PbS) containing 0.04 at.% Ag and Sb, 0.06 at.% Cu, 0.07 at.% Zn, and 0.08 at.% Au in silica ampoules. Mixtures of constituent elements in stoichiometric proportions (with an accuracy of 5×10^{-7} kg) were sealed into evacuated ampoules at the pressure of 10^{-3} Torr. The evacuated tube was then placed into an electric furnace and kept at 730 K for 7 days and after that at 970 K for 10 days. In order to avoid explosions due to the sulfur vapor pressure, the tube was heated slowly (300 K/h). The tubes were cooled gradually, with a cooling rate of about 295 K/h to room temperature in order to obtain polycrystalline $\text{Sn}_{1-x}\text{Pb}_x\text{S}$ compounds.

The main feature of the hot wall deposition system is the heated linear quartz tube of 1.2×10^{-2} m diameter, which served to enclose and direct the vapor from the source to the substrate. The quartz tube and substrates were heated independently. The quartz tube was charged with $\text{Sn}_{1-x}\text{Pb}_x\text{S}$ powder and the films were deposited by keeping the quartz tube temperatures around 870 K. Glass plates were chemically cleaned, rinsed with distilled water before deposition. Substrate temperature was varied from 520 to 680 K. The substrate was held at a distance of about 10^{-4} m above the open end of the quartz tube acting almost

as a lid closing the tube with the help of a substrate holder heater. The pressure in the chamber was about 10^{-5} Torr during evaporation. Chromel–alumel thermocouples were used to measure the temperatures of quartz tube and the substrate.

The crystal structure of the $\text{Sn}_{1-x}\text{Pb}_x\text{S}$ in both powder and thin film forms were investigated by X-ray diffraction (XRD) using a Siemens D-5000 diffractometer with $\text{CuK}\alpha$ ($\lambda = 1.5418 \text{ \AA}$) radiation. Silicon powder suspended in acetone and covering the samples was used as a standard. The 2Θ -range for the diffractometer was set from 10 to 100° with a step size of 0.038° . The observed phases were determined by comparing the d -spacing with the Joint Committee on Powder Diffraction Standard (JCPDS) data files. Surface morphology and cross-section of the films were investigated with scanning electron microscope (SEM) (Hitachi S-806). The elemental composition of the obtained films was determined from energy dispersive X-ray (EDX) data, using Scanning electron microscope Stereoscan-360 with EDX spectrometer AN 10000 with an accuracy of about 2 %. The depth profiling was done by Auger electron spectroscopy (AES) using a Perkin Elmer Physical Electronics model 590 with simultaneous sputter etching. The nature of the crystalline surface was also analyzed using atomic force microscopy (AFM, Model: NT-206) and the grain size was evaluated. The TEM examinations have been performed by means of a Philips CM-200 STEM operating at 200 kV accelerating voltage and equipped with a calibrated EDX system. The cross-sections needed for TEM were prepared by mechanical grinding, dimpling and Ar^+ ion milling using a Gatan PIPS machine.

Electrical conductivity measurements were made by using a dc two-probe configuration in a special cryostat. The temperature range of investigation was extended from 150–420 K. All measurements were carried out under vacuum condition of about 5×10^{-4} Torr. The “Leit-C” paste was used as ohmic contact. The ohmic nature of the contacts was checked by recording the current–voltage characteristics.

3. Results and discussion

The physical properties of $\text{Sn}_{1-x}\text{Pb}_x\text{S}$ thin films are influenced by the elemental composition and substrate temperature. The characteristics of layers were studied by appropriate techniques and are discussed in the following section. The as-deposited films were pinhole free and strongly adherent to the surface of the substrate. $\text{Sn}_{1-x}\text{Pb}_x\text{S}$ layers appeared grey in color; the valuated thickness varied from 2.0 to 4.0 μm .

The influence of substrate temperature and Pb content on the phase formation and crystalline structure of the $\text{Sn}_{1-x}\text{Pb}_x\text{S}$ structures were characterized by XRD measurements. Teallite pattern (PDF # 44-1437) was used as reference for qualitative analysis of the samples. The structures obtained were single phase in nature and had an orthorhombic crystal structure. All films showed strong orientation along [001] axes with strong 004 peak [24]. A linear relationship between the lattice parameters and the composition of $\text{Sn}_{1-x}\text{Pb}_x\text{S}$ thin films were established. These relationships, calculated mathematically by least-squares analysis, are:

$$a = 4.333 - 0,0745 \cdot x(\text{\AA}), \quad b = 3,977 + 0,1435 \cdot x(\text{\AA}), \quad c = 11,219 + 0,4402 \cdot x(\text{\AA}).$$

The value of the a parameter gradually decreases with increasing Pb content in films, while value of the b and c parameters increase and agree with data of previously synthesized herzenbergite–teallite bulk minerals [6]. The change of lattice parameters with substrate temperature is marginal. SEM examinations (Fig. 1) of the as-grown structures showed that the nanorods lawn was formed onto a thin film interlayer (about 1500 nm thick) on the glass substrate.

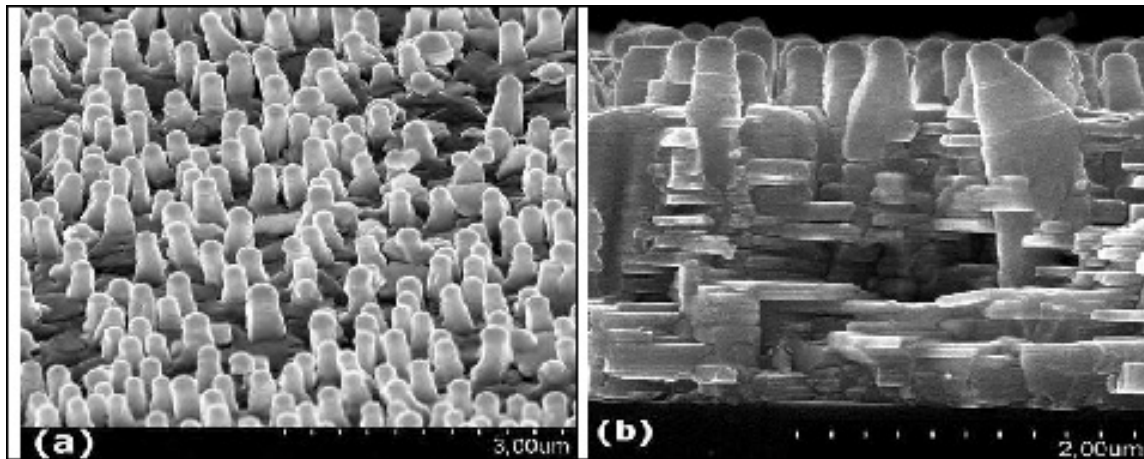


FIG. 1. SEM images of $\text{Sn}_{0.92}\text{Pb}_{0.08}\text{S}$ nanorods grown onto underlying thin film (a) top view, (b) cross sectional view

The average length and diameter of rods for the $\text{Sn}_{0.92}\text{Pb}_{0.08}\text{S}$ sample are 500 nm and 250 nm respectively. The underlying thin film is composed by single-crystalline blocks with their orthorhombic 11.2 Å axis (c-axis) always perpendicular to the substrate surface (Fig. 2).

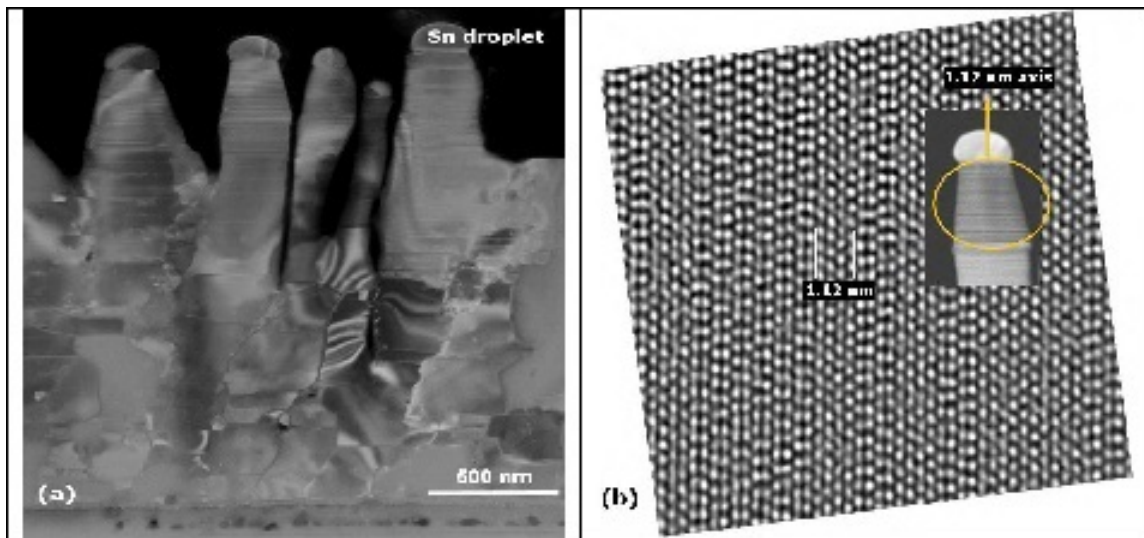


FIG. 2. (a) TEM bright-field image of nanorods and block structured underlying thin film of $\text{Sn}_{0.92}\text{Pb}_{0.08}\text{S}$, (b) bragg-filtered experimental HRTEM image of plane defects

The individual adjacent blocks, which differ in their azimuthal orientation, are randomly directed. Therefore, the whole grown $\text{Sn}_{1-x}\text{Pb}_x\text{S}$ displays polycrystalline behavior but has a well-distinct (001) texture, which is in agreement with XRD results [24]. However, between blocks that are stacked over each other to form columns there are well-defined twist boundaries. The whiskers are formed either by thicker blocks (see Fig. 2,b) separated by twist boundaries containing dislocations or they are composed of many extremely thin lamellae with the same orientation relationship as the blocks but without dislocations. This means that in the former case, plastic relaxation between stacked blocks took place. In the

latter one, pseudomorphic intergrowth between stacked thin strained lamellae occurs, i.e., there is elastic relaxation without forming dislocations. As revealed by TEM-EDX analysis, the average composition of the blocks and rods is the same without any composition gradient across the whole $\text{Sn}_{1-x}\text{Pb}_x\text{S}$ sample structure (Fig. 3). As seen from the Fig. 1 and Fig. 2 the droplets were formed at the tip of the rods. TEM-EDX experiments showed that these droplets consist of Sn and about 0.6 at.% Pb and 1.2 at.% S.

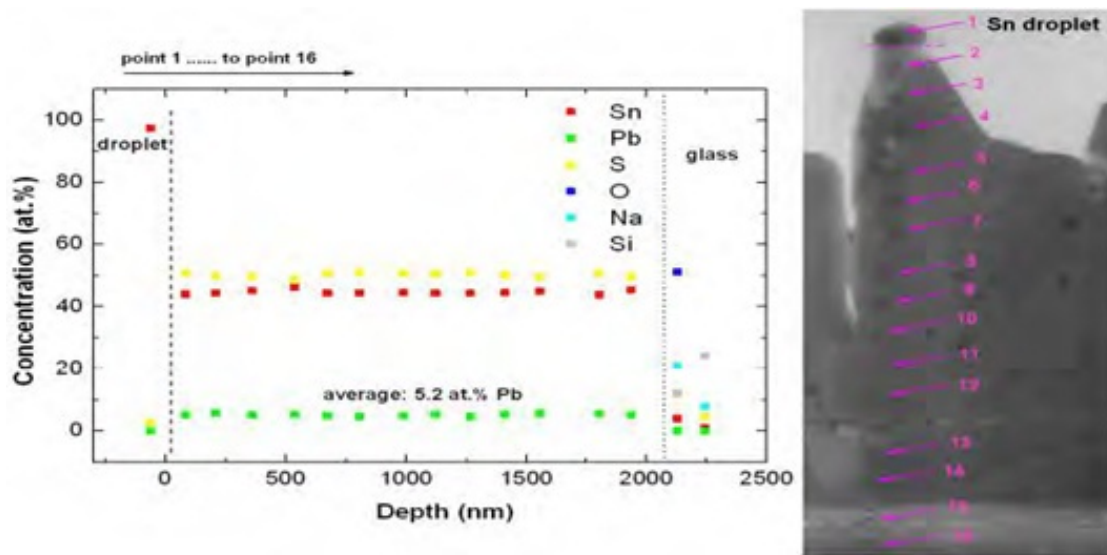


FIG. 3. Compositional distribution along $\text{Sn}_{0.9}\text{Pb}_{0.1}\text{S}$ sample determined by calibrated TEM-EDX. The points for quantitative TEM-EDX measurements are indicated by 1 to 16

It was suggested that these droplets are liquid at growth temperature and act as a solute for the sulfur and lead, and tin may also come from the vapor phase during the growth process. Therefore, it is assumed the rods grew via a self-consuming vapor–liquid–solid (VLS) mechanism [13-14].

The experiments confirm that the nanorod growth depends strongly on the lead concentration and substrate temperature. The lawn of nanorods with lead concentration ranging from 4 at.% to 6 at.% was formed onto the underlying $\text{Sn}_{1-x}\text{Pb}_x\text{S}$ thin film at substrate temperatures of 570–590 K. Thin films containing ca. 8 at.% Pb grown on glass at temperatures less than 540 K have few droplets on their surfaces only (Fig. 4).

At a substrate temperature of 600 K, the droplets required for VLS growth begin to form (Fig. 4b) and at 630 K an array of whiskers 500 nm high and 250 nm in diameter can be observed (Figs. 4c). However, at substrate temperatures of 670 K and higher, lawn-growth could not be found even though some few droplets and single nanorods appeared. Thus, it can be concluded that for higher Pb content, higher substrate temperatures are required to produce nanorods. The as-grown $\text{Sn}_{1-x}\text{Pb}_x\text{S}$ films showed p-type electrical conductivity, which is confirmed by the thermoelectric probe measurement. The Seebeck coefficient and conductivity of the layers was in the range of $\alpha = 6\text{--}360 \mu\text{V}/\text{K}$ and $\sigma = 4.8 \times 10^{-5} - 1.5 \times 10^{-2} \Omega^{-1} \cdot \text{cm}^{-1}$ respectively at room temperature, depending on concentration of the lead in the films.

An increase of the Pb concentration leads to a decrease of the Seebeck coefficient and decrease of conductivity [4]. If Na deriving from diffusion from the glass substrate is

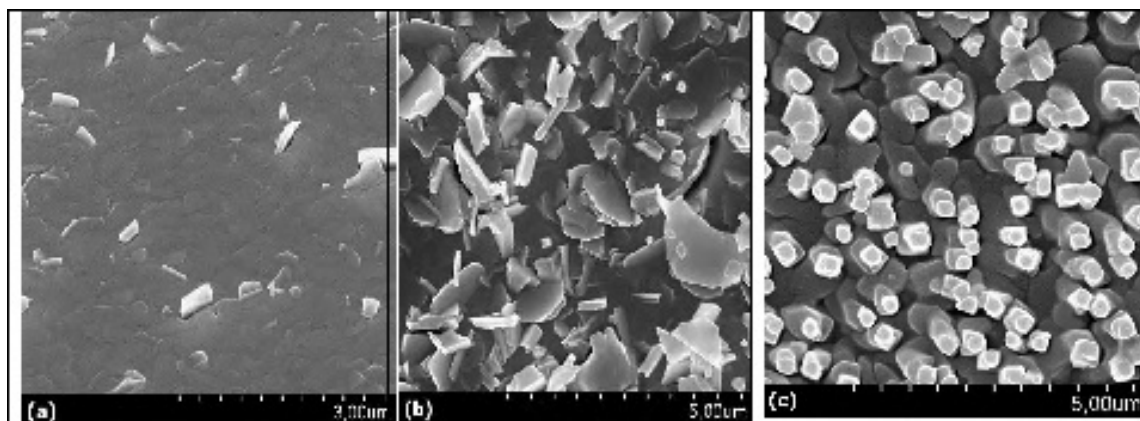


FIG. 4. SEM images of $\text{Sn}_{0.84}\text{Pb}_{0.16}\text{S}$ thin film samples deposited at different substrate temperature: (a) 540 K; (b) 600 K; (c) 630 K

incorporated within the thin film and nanorods, the electrical conductivity can be increased up to $\sigma = 10^2 \Omega^{-1}\cdot\text{cm}^{-1}$ and the Seebeck coefficient up to about $800 \mu\text{V}/\text{K}$. First data on structural and electrical characteristics of $\text{Sn}_{1-x}\text{Pb}_x\text{S}$ thin films grown by hot wall vacuum deposition method promise optimal conditions for application within photovoltaic and thermoelectrical devices.

4. Conclusion

$\text{Sn}_{1-x}\text{Pb}_x\text{S}$ films and nanorods were deposited by hot wall vacuum technique on glass substrates at temperatures of 520–680 K. The nanorods and film it self are composed of well-defined stacked blocks with orthorhombic crystal structure like $\alpha\text{-SnS}$ and show a preferential orientation along [001] perpendicular to the substrate surface. There is no composition gradient across the rods and the underlying thin film. Nanorod growth strongly depends on the lead concentration and substrate temperature. Increasing the Pb content requires the substrate temperature to be increased in order to realize whisker growth via VLS. Electrical measurements showed that $\text{Sn}_{1-x}\text{Pb}_x\text{S}$ films were of p-type conductivity. The values of Seebeck coefficient and conductivity at room temperature depended on the lead concentration were in the range of $6\text{--}360 \mu\text{V}/\text{K}$ and $4.8 \times 10^{-5} - 1.5 \times 10^{-2} \Omega^{-1}\cdot\text{cm}^{-1}$ respectively.

Acknowledgments

We acknowledge PD Dr. G. Wagner (Leipzig University) for TEM investigations and A. Bernstein (LMU München) for the EPMA analyses of natural PbS. This work has been supported by Belarusian Republican Foundation for Fundamental Research.

References

- [1] Razykov T.M. Solar photovoltaic electricity: Current status and future prospects. *Solar Energy*, **85**, P. 1580–1608 (2011).
- [2] Versavel M.Y., Haber J.A. Lead antimony sulfides as potential solar absorbers for thin film solar cells. *Thin Solid Films*, **515**, P. 5767–5770 (2007).
- [3] Dittrich H., Bieniok A., Brendel U., Grodzicki M. A new class of compound semiconductors for photovoltaic applications. *Thin Solid Films*, **515**, P. 5745–5750 (2007).
- [4] Unuchak D.M., Bente K., Kloess G., Schmitz W., Gremenok V.F., Ivanov V.A., Ukhov V. Structure and optical properties of PbS-SnS mixed crystal thin films. *Physics Status Solidi C*, **6**, P. 1191–1194 (2009).

- [5] Krebs H. and Langner D. Über struktur und eigenschaften der halbmatalle. XVI. Mischkristallsysteme zwischen halbleitenden chalcogeniden der vierten hauptgruppe. *Zeitschrift für anorganische und allgemeine Chemie*, **334**, P. 37–49 (1964).
- [6] Hayashi K., Kitakaze A., Sugaki A. A re-examination of herzenbergite-teallite solid solution at temperatures between 300 and 700°C. *Mineralogical Magazine*, **65**, P. 645–651 (2001).
- [7] Lebedev A.I., Sluchinskaya I.A., Munro I.H. An EXAFS study of the local structure of the $\text{Pb}_x\text{Sn}_{1-x}\text{S}$ solid solution. *Physics of the Solid State*, **44**, P. 1643–1647 (2002).
- [8] Thangaraju B. and Kaliannan P. Polycrystalline Lead Tin Chalcogenide Thin Film Grown by Spray Pyrolysis Crystal Research Technology, **35**, P. 71–75 (2000).
- [9] Lieber C.M. One-Dimensional Nanostructures: Chemistry, Physics & Applications. *Solid State Communications*, **107**, P. 607–616 (1998).
- [10] Manna L., Scher E.C., Alivisatos A.P. Synthesis of soluble and processable rod-, arrow-, teardrop-, and tetrapod-shaped CdSe nanocrystals. *J. American Chemistry Society*, **122**, P. 12700–12706 (2000).
- [11] Deng Z.X., Wang C., Sun X.M., Li Y.D. Structure-Directing Coordination Template Effect of Ethylenediamine in Formations of ZnS and ZnSe Nanocrystallites via Solvothermal Route. *Inorganic Chemistry*, **41**, P. 869–873 (2002).
- [12] Rao C.N., Deepak F.L., Gundiah. G., Govindaraj A. Inorganic nanowires. *Progress Solid State Chemistry*, **31**, P. 5–147 (2003).
- [13] Xia Y.N., Yang P.D., Sun Y.G., Wu Y.Y., Mayers B., Gates B., Yin Y.D., Kim F., Yan H.Q. One-Dimensional Nanostructures: Synthesis, Characterization, and Applications. *Advanced Materials*, **15**, P. 353–389 (2003).
- [14] Wagner R.S., Ellis W.S. Vapor-liquid-solid mechanism of single crystal growth. *Applied Physics Letters*, **4**, P. 89–90 (1964).
- [15] Lopez-Otero, A. Hot wall epitaxy. *Thin Solid Films*, **49**, P. 3–57 (1978).
- [16] Chaudhuri S., Mondal A., Pal A.K. Structural studies of CdSe films deposited onto glass, NaCl and substrates by a hot-wall technique. *Journal of Materials Science Letters*, **6**, P. 366–369 (1987).
- [17] Seto S., Yamada S., Suzuki K. Growth kinetics and structural characterization of polycrystalline CdTe films grown by hot-wall vacuum evaporation. *Solar Energy Materials and Solar Cells*, **50**, P. 133–139 (1998).
- [18] Velumani S., Narayandass S.K., Mangalara D. Structural characterization of hot wall deposited cadmium selenide thin films. *Semiconductors Science and Technology*, **13**, P. 1016–1024 (1998).
- [19] Velumani, S., Mathew, X., Sebastian, P.J. Thickness dependent properties of hot wall deposited CdSe films. *Journal of Materials Science Letters*, **22**, P. 25–28 (2003).
- [20] Muthukumarasamy N., Balasundaraprabhu R., Jayakumar S., Kannan M.D. Photoconductive properties of hot wall deposited $\text{CdSe}_{0.6}\text{Te}_{0.4}$ thin films. *Materials Science and Engineering B*, **137**, P. 1–4 (2007).
- [21] Agilan S., Venkatachalam S., Mangalaraj D., Narayandass Sa.K., Velumani S., Singh Vijay P. Structural and photoelectrical characterization of hot wall deposited CuInSe_2 thin films and the fabrication of CuInSe_2 based solar cells. *Materials Characterization*, **58**, P. 701–707 (2007).
- [22] Schikora D., Sitter H., Humenberger J., Lischka K. High quality CdTe epilayers on GaAs grown by hotwall epitaxy. *Applied Physics Letters*, **48**, P. 1276–1278 (1986).
- [23] Pal A.K., Mondal A., Chaudhuri S. Preparation and characterization of ZnTe/CdSe solar cells. *Vacuum*, **41**, P. 1460–1462 (1990).
- [24] Bente K, Lazenka V.V., Unuchak D.G., Wagner G., Gremenok V.F. Epitaxial $\text{Sn}_{1-x}\text{Pb}_x\text{S}$ nanorods on iso-compositional thin films, Crystal. *Research Technology*, **45**, P. 643–646 (2010).